# Effects of Formation Epoch Distribution on X-Ray Luminosity and Temperature Functions of Galaxy Clusters

Motohiro Enoki <sup>1,2</sup>, Fumio Takahara <sup>1</sup>, and Yutaka Fujita <sup>2</sup>

## ABSTRACT

We investigate statistical properties of galaxy clusters in the context of hierarchical clustering scenario, taking account of their formation epoch distribution, motivated by the recent finding by Fujita and Takahara that X-ray clusters form a fundamental plane, where the mass and formation epoch are regarded as two independent parameters. Using the formalism which discriminates between major merger and accretion, the epoch of a cluster formation is identified with that of the last major merger. Since tiny mass accretion after the formation does not much affect the core structure of clusters, the properties of X-ray emission from clusters are determined by the total mass and density at their formation time. Under these assumptions, we calculate X-ray luminosity and temperature functions of galaxy clusters. We find that the behavior of luminosity function is different from the model which does not take account of formation epoch distribution, while the behavior of temperature function is not much changed. In our model, luminosity function is shifted to a higher luminosity and shows no significant evolution up to  $z \sim 1$ , independent of cosmological models. The clusters are populated on the temperature-luminosity plane with a finite dispersion. Since the simple scaling model in which the gas temperature is equal to the virial temperature fails to reproduce the observed luminosity-temperature relation, we also consider a model which takes the effects of preheating into account. The preheating model reproduces the observations much better.

Subject headings: cosmology: theory — clusters: galaxies: general — X-rays: galaxies

## 1. Introduction

Galaxy clusters are the largest virialized objects in the universe and should be useful cosmological probe since the properties of clusters are considered to depend on cosmological parameters

<sup>&</sup>lt;sup>1</sup>Department of Earth and Space Science, Graduate School of Science, Osaka University, Toyonaka, Osaka, 560-0043, Japan

<sup>&</sup>lt;sup>2</sup>National Astronomical Observatory, Osawa 2-21-1, Mitaka, Tokyo, 181-8588, Japan

and to reflect the structure formation history. Galaxy clusters contain a diffuse hot gas which emits X-rays via thermal bremsstrahlung. The X-ray temperature and luminosity functions of clusters and their evolution have been used to determine the density of the universe and the amplitude of the rms density fluctuation. If there exist unique mass-temperature (T) and mass-luminosity (L)relations, one can predict X-ray temperature and luminosity functions of clusters at redshift z from a theoretical mass function. Therefore, it is important to investigate into correlations among physical quantities of clusters and examine if such unique relations exist. Recently, Fujita & Takahara (1999a) have found that clusters at low redshifts (z < 0.1) form a plane (the fundamental plane) in the three dimensional space (log  $\rho_{\text{gas},0}$ , log  $r_c$ , log T), where  $\rho_{\text{gas},0}$  is the central gas density, and  $r_c$ is the core radius of clusters. The data on the plane still have a correlation and form a band on the plane. The observed relation  $L \propto T^3$  turns out to be the cross section of the band normal to the major axis. The existence of the fundamental plane implies that the clusters form a two-parameter family, suggesting that the physical quantities of clusters are determined by the halo mass and density at the time of their formation and that no unique mass-temperature or mass-luminosity relation exists (Fujita & Takahara 1999b). In fact, using N-body simulations, Navaro, Frenk, & White (1997) found that the structure of clusters is related to their formation epoch, although they claimed that the clusters are a one-parameter family by assuming a unique relation between the mass and formation redshift. In this paper, motivated by the finding of the fundamental plane, we present a formulation of statistics of clusters in the context of hierarchical structure formation theory taking account of formation epoch distribution.

So far, Press & Schechter (1974, hereafter PS) mass function has been widely used to calculate temperature and luminosity functions (e.g. Eke, Cole, & Frenk 1996). Although PS mass function provides the number of dark halos at a given time, it does not contain information about the formation time of halos. Thus, a conventional way to compute the temperature and luminosity functions is simply to assume that the formation time is the same as the observed time. Since in this case clusters form a one-parameter family about the mass, an extension of PS theory is necessary to investigate the two-parameter nature of clusters, taking account of the effect of the formation epoch distribution. Using the merger probabilities in an extended Press & Schechter clustering model (Bond et al. 1991; Bower 1991), Lacey & Cole (1993, hereafter LC) derived a formation epoch distribution function in an enlightening way, although LC did not calculate predictions of X-ray luminosity and temperature functions. The formation time in their model is defined by that time when the halo mass becomes half that at the observed epoch and this definition does not discriminate between tiny and notable relative mass capture, or between accretion and merger. In the hierarchical clustering scenario, low-mass objects successively merge with one another to build up ever more massive objects. However, major deviations from equilibrium and subsequent relaxation take place only when halos of comparable masses merge, while tiny mass captures have little effect on the capturing halos. So, it is desirable to devise such formulations. Kitayama & Suto (1996a,b) have attempted to describe the formation and destruction of halos within the extended PS prescription by discriminating between accretion and merger. They define the halo formation and destruction rates and define the formation epoch distribution by utilizing the survival probability. Although they predict various statistical properties of X-ray clusters, they assume an empirical relation between temperature and luminosity in such predictions, which is not satisfactory from our point of view.

In this paper, we adopt another model of the formation epoch distribution proposed by Salvador-Solé, Solanes & Manrique (1999, hereafter SSM). They developed a modification of the extended PS model that differentiates merger from accretion and define the formation epoch as the epoch of the last major merger by utilizing the empirical mass-density correlation obtained by N-body simulations. Following this formalism, we can obtain not only formation time distribution but also the halo mass at the formation time. In order to obtain statistics of galaxy clusters, we assume that the halo mass and density at its last major merger determine the structure of clusters. The temperature and luminosity of galaxy clusters are calculated in terms of the halo mass and density at the formation without resorting to empirical relations. On the basis of these prescriptions, we construct a simple scaling model of X-ray clusters and calculate L - T distribution, the temperature and luminosity functions. Since it is well known that a simple scaling model between gas and dark matter results in an L - T relation different from observations (Eke, Navarro, & Frenk 1998), we also investigate a simple preheating model. The paper is organized as follows. The formulation of statistics is presented in § 2. The X-ray cluster model is constructed in § 2.2. The results and discussion are described in § 3.

#### 2. Formulation

#### 2.1. Formation time distribution

In this subsection, we summarize the SSM formalism. To follow the formation and evolution of halos, SSM used a modified version of the extended PS clustering model (Bond et al. 1991; Bower 1991, ; LC) and made a schematic distinction between minor and major mergers by defining the formation of a halo as the last major merger it experienced. This definition does not affect the abundance of halos at a given time, although it affects the description of their growth. Thus, the mass function is equal to the PS mass function

$$n(M,t)dM = \sqrt{\frac{2}{\pi}} \frac{\rho_0}{M} \frac{\delta_c(t)}{\sigma^2(M)} \left| \frac{d\sigma(M)}{dM} \right| \exp\left[ -\frac{1}{2} \frac{\delta_c^2(t)}{\sigma^2(M)} \right] dM,\tag{1}$$

where  $\rho_0$  is the present mean density of the universe,  $\delta_c(t)$  is the critical density contrast for collapse at t, and  $\sigma(M)$  is the rms density fluctuation in spheres containing a mean mass M. In this paper, we use an approximate formula of  $\delta_c(t)$  for spatially flat cosmological model (Nakamura & Suto 1997) and a fitting formula of  $\sigma(M)$  for the CDM fluctuation spectrum (Kitayama 1997).

In the LC model, the instantaneous merger rate for halos with mass M at t per infinitesimal

range of final mass M' > M, or specific merger rate, is

$$r_{\rm LC}^m(M \to M', t) dM' \equiv \sqrt{\frac{2}{\pi}} \left| \frac{d\delta_c(t)}{dt} \right| \frac{1}{\sigma^2(M')} \left| \frac{d\sigma(M')}{dM'} \right| \\ \times \left[ 1 - \frac{\sigma^2(M')}{\sigma^2(M)} \right]^{-3/2} \\ \times \exp\left\{ -\frac{\delta_c^2(t)}{2} \left[ \frac{1}{\sigma^2(M')} - \frac{1}{\sigma^2(M)} \right] \right\} dM'.$$
(2)

In the SSM formalism, it is assumed that a halo with mass M experiences a major merger and is destroyed when the relative mass increment  $\Delta M/M \equiv (M' - M)/M$  exceeds a certain threshold  $\Delta_m$ . The major merger is regarded as the formation of a new halo. On the other hand, when  $\Delta M/M < \Delta_m$ , the event is regarded as continuous accretion; the halo keeps its identity and its core structure. Thus, from the specific merger rate (eq. [2]), the mass accretion rate,  $R_{\text{mass}}(M, t) \equiv dM/dt$ , of halos with mass M at time t is defined as

$$R_{\rm mass}(M,t) = \int_{M}^{M(1+\Delta_m)} \Delta M r_{\rm LC}^m(M \to M',t) dM'.$$
(3)

The destruction rate is defined as

$$r^{d}(M,t) = \int_{M(1+\Delta_{m})}^{\infty} r_{\rm LC}^{m}(M \to M',t) dM'.$$
(4)

The formation rate should be written by

$$r^{f}[M(t),t] = \frac{d\ln n[M(t),t]}{dt} + r^{d}[M(t),t] + \partial_{M}R_{\text{mass}}[M(t),t]$$
(5)

from the conservation equation for the number density of halos per unit mass along mean mass accretion tracks, M(t), which is the solution of the differential equation

$$\frac{dM}{dt} = R_{\rm mass}[M(t), t]. \tag{6}$$

From this formation rate, one can obtain the distribution of formation time,  $t_f$ , for halos with masses M at t;

$$\Phi_f(t_f; M, t) dt_f = r^f[M(t_f), t_f] \exp\left\{-\int_{t_f}^t r_f[M(t'), t'] dt'\right\} dt_f.$$
(7)

From equation (6), the halo mass at formation time,  $M_f = M(t_f)$ , becomes

$$M_f = M - \int_{t_f}^t R_{\text{mass}}[M(t'), t']dt'.$$
 (8)

The value of  $\Delta_m$  is fixed by the fits to the empirical mass-density (or mass-radius) correlation obtained by N-body simulations (Navaro, Frenk, & White 1996, 1997). The best fit is  $\Delta_m = 0.6$ in a number of different cosmological models (SSM). To be precise,  $M_f$  for fixed M and  $z_f$  should have scatter around the mean accretion track (eq. [6]). Therefore,  $M_f$  in equation (8) is an approximation to the mean formation mass of true distribution. Although we ignore this scatter for the sake of simplicity, it could be estimated by using the algorithm given in Nusser & Sheth (1999).

In this paper, we investigate two cosmological models (SCDM and LCDM). In Table 1, we tabulate the cosmological density parameter ( $\Omega_0$ ), the cosmological constant ( $\lambda_0$ ), the Hubble constant in units of 100 km s<sup>-1</sup> Mpc<sup>-1</sup> (h), and the present rms density fluctuation in spheres of radius  $8h^{-1}$ Mpc ( $\sigma_8$ ). Figure 1 shows the formation time distributions (eq. [7]) for the SCDM and LCDM models for several values of the present halo mass. Since in the LCDM model the universe is in the accelerated expanding stage at  $z \sim 0$ , the growth of density fluctuation has stopped. Thus, the slope of the formation time distribution in the LCDM model is less steep in comparison with the SCDM model at  $z \sim 0$  (Figure 1). Figure 2 shows halo masses at its formation time (eq. [8]) for the halo with the present mass of  $10^{15} M_{\odot}$ .

Note that, in the PS formalism, there is no distinction between merger and accretion. Any mass capture is regarded as merger, that is,  $t_f = t$ . Consequently, the formation time distribution is

$$\Phi_f(t_f; M, t) = \delta^D(t_f - t) , \qquad (9)$$

where  $\delta^D(x)$  is Dirac's delta function.

#### 2.2. X-ray cluster model

In the SSM formalism, the mass function of dark halos at a fixed epoch is given by the PS mass function. On the other hand, for a given mass, the dark halos take a range of formation time as depicted by equation (7). Thus, dark halos form a two-parameter family. SSM found that the characteristic density and the scale radius of a halo at the present epoch are proportional to the critical density of the universe and the virial radius of the halo at the formation time  $t = t_f$ , respectively. This means that, between major mergers, halos gradually grow through the accretion of surrounding matter while keeping the central part unchanged. Considering the two-parameter family nature of clusters, we thus assume that the physical quantities of clusters of galaxies are represented by the mass and the virial density at the their formation time or the last major merger. On this assumption, the temperature and luminosity of a cluster are determined by the formation redshift  $z_f$  and the halo mass  $M_f$  at  $z_f$ ;  $T = T[z_f, M_f(M, z_f)]$ ,  $L = L[z_f, M_f(M, z_f)]$ . Here, the relation between  $t_f$  and  $z_f$  are straightforwardly determined once the cosmological model is specified. In order to obtain L and T, we use the spherical collapse model (Tomita 1969; Gunn & Gott 1972) and assume that the cluster is spherically symmetric and intracluster gas is in an

isothermal hydrostatic equilibrium in the gravitational potential of dark matter halo.

In the spherical collapse model, the virial density  $\rho_f$  of a halo at the formation redshift  $z_f$  is given by

$$\rho_f = \rho_c(z_f) \Delta_c(z_f) = \rho_{c0} \Delta_c(z_f) \frac{\Omega_0 (1+z_f)^3}{\Omega(z_f)},$$
(10)

where  $\rho_c(z_f)$  is the critical density of the universe,  $\Delta_c(z_f)$  is the ratio of the virial density to the critical density, and  $\Omega(z_f)$  is the cosmological density parameter. The index 0 refers to the values at z = 0. We use the fitting formula of Bryan & Norman (1998) for the virial density of spatially flat cosmological models;

$$\Delta_c = 18\pi^2 + 82x - 39x^2 , \qquad (11)$$

where  $x \equiv \Omega(z_f) - 1 = (\Omega_0 - 1) / [\Omega_0 (1 + z_f)^3 + 1 - \Omega_0].$ 

The virial radius is obtained by

$$r_f = \left(\frac{3M_f}{4\pi\rho_f}\right)^{1/3}.$$
(12)

The virial temperature  $T_{\rm vir}$  is given by

$$k_B T_{\rm vir} = \frac{\mu m_p G M_f}{3r_f} = 0.92 \left(\frac{M_f}{10^{15} M_{\odot}}\right)^{2/3} \left[h^2 \Delta_c \frac{\Omega_0}{\Omega(z_f)}\right]^{1/3} (1+z_f) \text{ keV}$$
(13)

where  $\mu$  is the mean molecular weight which we take to be  $\mu = 0.6$ ,  $m_p$  is the proton mass, and  $k_B$  is the Boltzmann constant.

The luminosity of a cluster is

$$L = 6.50 \times 10^{-24} \left(\frac{k_B T}{1 \text{keV}}\right)^{1/2} \int_0^{r_f} n_e^2 4\pi r^2 dr \text{ erg s}^{-1}$$
(14)

where  $n_e$  is the electron number density in CGS units. Note that the gas temperature T is not equal to the virial temperature  $T_{\rm vir}$  in general. In order to calculate luminosity from equation (14), we need to specify the gas density profile. Here, we adopt isothermal  $\beta$  model

$$\rho_{\rm gas}(r) = \rho_{\rm gas,0} \left[ 1 + \left(\frac{r}{r_c}\right)^2 \right]^{-3\beta/2},\tag{15}$$

where  $\rho_{\text{gas},0}$  is the central gas density and  $r_c$  is core radius. The central gas density is calculated through the relation

$$\int_0^{r_f} \rho_{\rm gas}(r) 4\pi r^2 dr = M_{\rm gas} \tag{16}$$

where  $M_{\text{gas}}$  is the total gas mass. From now on, we assume that  $r_c = r_f/8$  (Fujita & Takahara 1999b).

Thus, from (14) and (15), the luminosity is given by

$$L = 1.79 \times 10^{44} \left(\frac{k_B T}{1 \text{keV}}\right)^{1/2} \left(\frac{M_f}{10^{15} M_{\odot}}\right) \left[h^2 \Delta_c \frac{\Omega_0}{\Omega(z_f)}\right] (1+z_f)^3 f_m^2 \text{ erg s}^{-1}$$
(17)

where  $f_m \equiv M_{\text{gas}}/M_f$  is the gas mass fraction and we assume here  $\beta = 2/3$  for simplicity. Equations (13) and (17) show that the temperature and luminosity are functions of the halo mass and the formation redshift indeed when one specifies the cosmological model and the relation between T and  $T_{\text{vir}}$ .

## 2.3. Temperature and luminosity function

Next, we formulate statistics of galaxy clusters. Now that the temperature and luminosity are expressed as functions of  $t_f$  and  $M_f$ , such that  $T = T[t_f, M_f(M, t_f)]$  and  $L = L[t_f, M_f(M, t_f)]$ , we can derive temperature and luminosity functions using the transformation of the two variables from  $(t_f, M)$  to (T, L) as follows.

For a mass range  $M \sim M + dM$  at t, the comoving number density of clusters formed at  $t_f \sim t_f + dt_f$  is given by

$$n(t_f, M; t)dt_f dM = n(M; t)\Phi_f(t_f; M, t)dt_f dM.$$
(18)

Thus the comoving number density of clusters at t with  $T \sim T + dT$  and  $L \sim L + dL$  is given by

$$n(T,L;t)dTdL = n(t_f,M;t)dt_f dM.$$
(19)

Accordingly,

$$n(T,L;t) = n(t_f,M;t) \left| \frac{\partial(t_f,M)}{\partial(T,L)} \right|.$$
(20)

Since the comoving number density n(T, L; t) gives the distribution function on L - T plane, it reflects L - T relation of clusters.

The temperature function and luminosity function are respectively given by

$$n(T;t) = \int n(T,L;t)dL$$
(21)

and

$$n(L;t) = \int n(T,L;t)dT.$$
(22)

It is to be noted that these functions take account of the distribution of cluster formation time,  $t_f$ .

Thus, given the relations  $T = T[t_f, M_f(M, t_f)]$  and  $L = L[t_f, M_f(M, t_f)]$ , one can calculate the L - T distribution function, the temperature function and the luminosity function.

## 3. Results and discussion

In this section, we derive the temperature function, the luminosity function and L - T distribution function. We assume that the gas mass fraction of clusters  $f_m$  is the same as the cosmic baryon ratio  $\Omega_b/\Omega_0$  where  $\Omega_b$  is the density parameter of baryon and we adopt  $\Omega_b = 0.0125h^{-2}$  to be consistent with the primordial nucleosynthesis.

## 3.1. Scaling model

First, we examine the case where the gas temperature T is equal to the virial temperature  $T_{\rm vir}$ . In this case, the structure is self-similar and we call this model the scaling model. We calculate the temperature and luminosity functions based on the SSM formalism (eq. [7]) and compare them with those based on the PS formalism (eq. [9]). The temperature function and their redshift evolution are shown in Figure 3, where thin lines and symbols denote SSM and PS predictions, respectively. As is seen, there is little difference between the predictions of the two formalisms. This can be explained as follows. When we take account of the distribution of the formation time, physical quantities of clusters are affected by two factors. First, if the object formed earlier, its virial density becomes larger (eq. [10]). Second, if the object formed earlier, its mass at the formation becomes smaller for a given mass at z = 0 (Figure 2). Gas temperature depends on the virial density and mass at the formation time as  $T \propto M_f/r_f \propto \rho_f^{1/3} M_f^{2/3}$ , and these two factors tend to cancel out. This behavior of temperature function is the same as that of previous studies (e.g. Kitayama & Suto 1996b). This feature is common to both the cosmological models we investigate. The  $z_f$  dependence of temperature,  $T = T(z_f, M = 10^{15} M_{\odot})$ , is shown in Figure 4, which explicitly shows that T is roughly constant for  $z_f \lesssim 2$ . Note that Mathiesen (1999) also finds no evidence for a correlation between X-ray temperature and formation time in his simulation of X-ray clusters. The difference between SCDM model and LCDM model is mainly caused by the dependence on the time evolution of virial density (eq. [10]).

The luminosity function and their redshift evolution are shown in Figure 5, where thin lines and symbols denote SSM and PS predictions, respectively. As is seen, SSM formalism predicts larger number density than PS formalism and for the SSM formalism, there is little evolution even in SCDM model in contrast with the PS formalism. This result is different from that of the temperature function, because of the difference between the dependence of temperature and luminosity on the virial density and mass at the formation. Since  $L \propto \rho_f^2 r_f^3 T^{1/2} \propto \rho_f M_f T^{1/2} \propto \rho_f^{7/6} M_f^{4/3}$ , the luminosity depends more strongly on the virial density than the temperature. The  $z_f$  dependence of luminosity,  $L = L(z_f, M = 10^{15} M_{\odot})$ , is presented in Figure 6, which shows that L increases with  $z_f$ . Therefore, earlier formed dense clusters contribute to the increase of the luminosity function shown in Figure 5. Moreover, the increase of L with  $z_f$  explains that there is little evolution of the luminosity function from z = 1.0 to z = 0 both in SCDM and LCDM universes. Since the growth of density fluctuations in SCDM model is more rapid than that in LCDM model, one might think that the luminosity function in SCDM model should evolve rapidly. However, the present result implies that it is not the case if we consider the effect of the distribution in the formation redshift. Thus, recent observational evidence for little evolution of luminosity function (Rosati et al. 1998; De Grandi et al. 1999; Nichol et al. 1999) does not necessarily mean that SCDM model is disfavored against LCDM model. It is also noted that if we consider the effect of formation epoch distribution, smaller value of  $\sigma_8$  is needed to reproduce observations compared with the PS formalism.

When we compare the predictions with observations, one should note that the amplitude of temperature and luminosity functions can be adjusted by changing  $\sigma_8$  so that we are concerned with their shape. In Figure 3, the thick line is the best power-law fit to the observed low redshift temperature function obtained by Henry (2000). The predicted shape of the temperature function is consistent with observations both for SCDM and LCDM models, although agreement is better for LCDM model. In Figure 5 the thick line is the best fitted Schechter function to the observed bolometric luminosity function within z = 0.3 obtained by Ebeling et al. (1997). The predicted shape is much steeper than the observations both for SCDM and LCDM models. This is another representation of the well-known discrepancy of the L - T relation.

Next, we investigate the distribution on the L-T relation. For several values of  $n[\log(T), \log(L); z =$ 0], we plot iso-density contours on the L-T plane in Figure 7. From the relations  $T \propto \rho_f^{1/3} M_f^{2/3}$ and  $L \propto \rho_f^{7/6} M_f^{4/3}$ , the luminosity behaves as  $L \propto \rho_f^{1/2} T^2$ . As discussed in §1, in the PS formalism it is assumed that the observed redshift of a cluster is equal to the formation redshift  $(z = z_f)$ . Thus, most of the observed clusters  $(z \sim 0)$  have nearly the same virial density  $\rho_f(z)$  and their physical quantities depend only on mass. Therefore, in the PS formalism, clusters form a oneparameter family, which is shown by the straight line. On the other hand, in the SSM formalism. the virial densities take a wide range of values because  $\rho_f$  depends on the formation redshift. Thus, clusters form a two-parameter family. The scatter of the L-T relation shown in Figure 7 reflects the dispersion of the halo formation time. Scharf & Mushotzky (1997) also pointed this out. Since  $\rho_f$  tends to be distributed more widely for smaller clusters, the scatter of L-T relation is larger at lower T and L. Thus, the slope of L - T relation in the SSM formalism becomes shallower than  $L \propto T^2$ . This is, however, in conflict with the observed correlation  $L \propto T^3$  (e.g. David et al. 1993). As long as we assume that the ratio of the gas density of the core to the virial density is constant, this tendency persists. To resolve this discrepancy, this ratio should vary such that less massive clusters have smaller baryon fraction at the cluster core from which much of the X-ray emission originates (Metzler and Evrard 1994; Kay and Bower 1999; Valageas and Silk 1999; Wu, Fabian, & Nulsen 2000). Many authors have attributed such behavior to preheating of intracluster gas (Kaiser 1991; Evrard & Henry 1991; Cavaliere et al. 1998; Balogh et al. 1999), in which intracluster gas had already been heated before the cluster formed. On the other hand, some authors claimed that intracluster gas is heated after the formation of the cluster (Loewenstein 2000; Brighenti & Mathews 2001). Moreover, Bryan (2000) argued that cooling of gas and the resultant galaxy formation are sufficient to explain to lower the gas fraction in small clusters and groups without

additional heating. Since these models give qualitatively similar gas distributions, we will adopt a preheating model in the next subsection. It is to be noted future observations may discriminate the heating or galaxy formation models (e.g. Fujita 2001).

### 3.2. Preheating model

We examine the effects of preheating using a simple model of Fujita & Takahara (2000) based on the models of Cavaliere et al. (1998). They combine effects of shock heating and preheating so that the gas temperature is higher than the virial temperature such that

$$T = T_{\rm vir} + \frac{3}{2}T_1,$$
 (23)

where  $T_1$  is a given preshock temperature. In this model,  $\beta$  is given by

$$\beta = \frac{T_{\rm vir}}{T_{\rm vir} + (3/2)T_1}.$$
(24)

If  $T_1$  is not negligible compared to  $T_{\text{vir}}$ ,  $\beta$  becomes smaller, which means that hot gas expands and the gas density in the core decreases under the condition that the total gas mass of the cluster is constant. As a result, X-ray luminosity becomes smaller, which results in a steeper L - T relation. Comparison with observations of clusters suggests that the preheated temperature,  $T_1$ , is about 0.5 - 2 keV (Fujita & Takahara 2000). Here, we adopt  $T_1 = 1 \text{ keV}$ .

Using equation (15), we define the normalized central gas density as

$$f_d(\beta) \equiv \frac{\rho_{\text{gas},0}}{\rho_f} = \frac{4\pi f_m}{3I_1(\beta)} \left(\frac{r_f}{r_c}\right)^3 \,, \tag{25}$$

where

$$I_1(\beta) \equiv 4\pi \int_0^{r_f/r_c} \frac{x^2}{(1+x^2)^{3\beta/2}} dx.$$
 (26)

From equations (14), (15) and (25), the luminosity is written, using  $f_d(\beta)$ , as

$$L = 3.2 \times 10^{40} \left(\frac{k_B T}{1 \text{ keV}}\right)^{1/2} \left(\frac{M_f}{10^{15} M_{\odot}}\right) \left[h^2 \Delta_c \frac{\Omega_0}{\Omega(z_f)}\right] (1 + z_f)^3 f_d(\beta)^2 \ I_2(\beta) \text{ erg s}^{-1},$$
(27)

where we assume  $r_f/r_c = 8$ , and

$$I_2(\beta) \equiv 4\pi \int_0^8 \frac{x^2}{(1+x^2)^{3\beta}} dx.$$
 (28)

Because  $\beta$  is a function of  $T_{\text{vir}}$  once  $T_1$  is fixed,  $T \ L$  are function of  $z_f$  and  $M_f$  in this preheating model, as is the case of the scaling model. Thus, we can calculate the  $z_f$  dependences of the temperature and luminosity functions using the formulation constructed in § 2.3. The  $z_f$ 

dependence of temperature,  $T = T(z_f, M = 10^{15} M_{\odot})$ , and that of the luminosity,  $L = L(z_f, M = 10^{15} M_{\odot})$ , are shown by thick lines in Figures 4 and 6, respectively. Because of preheating, the gas temperature becomes higher and luminosity becomes lower compared with the scaling model predictions for this case. The temperature and luminosity functions are shown in Figures 8 and 9, respectively. For several values of  $n[\log(T), \log(L); z = 0]$ , iso-density contours on the L - T plane are plotted in Figure 10. Because of the preheating, the gas temperature is raised and the gas expands compared to the case without preheating. Thus, the central gas density,  $f_d$ , is decreased and luminosity is lowered. When  $T_{\rm vir} \sim T_1$ , the effect of preheating is large and luminosity is greatly decreased. On the other hand, when  $T_{\rm vir} \gg T_1$ , a cluster is not much affected by the preheating model is larger than that in the scaling model in spite of preheating. Therefore, the slope of L - T relation in the preheating model is steeper than  $L \propto T^2$  (Figure 10), the number of clusters with  $L > 10^{44} {\rm erg s}^{-1}$  increases (Figure 9), and the number of clusters with  $L < 10^{44} {\rm erg s}^{-1}$  decreases (Figure 9). In the preheating model, there is also little evolution of luminosity function. This reason is the same as the scaling model.

In Figures 8 and 9, the thick lines are the observed temperature and luminosity functions which are the same as Figure 3 and Figure 5. Both in the SCDM and LCDM model, the slope of the luminosity function based on the SSM formalism are near to the observed one, although it is still slightly steeper in the LCDM model. On the other hand, the slope of the temperature function is steeper than the observed one. Better data and better preheating models are needed to resolve this mismatch. In Figure 10, the thick solid lines show the PS prediction which becomes as steep as the observed slope because of the preheating effect. The thick dotted lines represent the observed L - T relation obtained by David et al. (1993). Note that observed L - T relation has a large dispersion which is comparable to the predicted width. Both in the SCDM and LCDM models, the predicted L - T relation can match the observed relation rather well.

#### 4. Conclusions

We have investigated the effects of formation epoch distribution on the statistical properties of galaxy clusters in the context of hierarchical structure formation scenario. The mass and formation redshift of galaxy clusters constitute two independent parameters. In this way, using the formalism of Salvador-Solé, Solanes & Manrique (1999), with a few plausible assumptions, we have derived temperature and luminosity functions and the distribution on the L-T plane. First, we investigated a simple scaling model in which gas temperature is equal to the virial temperature. The temperature function is almost the same as that in the PS formalism, while the luminosity function is shifted to higher luminosity and shows no significant evolution independent of the cosmological model because earlier formed clusters have denser intracluster gas in the cluster core. The luminosity-temperature relation becomes a band with a broad width instead of a linear line, but its slope becomes a little flatter than that of the PS formalism, which is inconsistent with the observations. Second, we have

examined a simple preheating model in this framework. Preheating makes the gas distributions of poor clusters flatter than those of rich clusters, which reduces the X-ray luminosity. The resultant L - T relation is steeper than that in the scaling model and becomes consistent with observations. Although the temperature and luminosity functions are broadly consistent with observations, too, better observations and better preheating models are needed for quantitative comparisons.

## REFERENCES

- Balogh, M., Babul, A., & Patton, D. R. 1999, MNRAS, 307, 463
- Bond, J. R., Cole, S., Efstathiou, G., & Kaiser, N. 1991, ApJ, 379, 440
- Bower, R. J. 1991, MNRAS, 248, 332
- Brighenti, F., & Mathews, W. G. 2001, ApJ, in press
- Bryan, G. L., & Norman, M. L. 1998, ApJ, 495, 80
- Bryan, G. L. 2000 ApJ, 544, L1
- Cavaliere, A., Menci, N., Tozzi, P. 1998, ApJ, 501, 493
- David, L. P., Slyz, A., Jones, C., Forman, W., & Vrtilek, S. D. 1993, ApJ, 412, 479
- De Grandi, S., Guzzo, L., Böhringer, H., Molendi, S., Chincarini, G., Collins, C., Cruddace, R., Neumann, D., Schindler, S., Schuecker, P., & Voges, W. 1999, ApJ, 513, L17
- Ebeling, H., Edge, A. C., Fabian, A. C., Allen, S. W., Crawford, C. S., & Böhringer, H. 1997, ApJ, 479, L101
- Eke, V. R., Cole, S., & Frenk, C. S. 1996, MNRAS, 282, 636
- Eke, V. R., Navarro, J. F., & Frenk, C. S. 1998, ApJ, 503, 569
- Evrard, A. E., & Henry, J. P. 1991, ApJ, 383, 95
- Fujita, Y. 2001, ApJLetters, in press (astro-ph/0102221)
- Fujita, Y., & Takahara, F. 1999a, ApJ, 519, L51
- Fujita, Y., & Takahara, F. 1999b, ApJ, 519, L55
- Fujita, Y., & Takahara, F. 2000, ApJ, 536, 523
- Gunn, J. E. & Gott, J. R. I. 1972, ApJ, 176, 1
- Henry, J. P. 2000, ApJ, 534, 565

- Kaiser, N. 1991, ApJ, 383, 104
- Kay, S. T., & Bower, R. G. 1999, MNRAS, 308, 664
- Kitayama, T., & Suto, Y. 1996a, MNRAS, 280, 683
- Kitayama, T., & Suto, Y. 1996b, ApJ, 469, 480
- Kitayama, T., 1998, PhD thesis, Univ. Tokyo
- Lacey, C. G., & Cole, S. 1993, MNRAS, 262, 627 (LC)
- Loewenstein, M. 2000, ApJ, 532, 17
- Mathiesen, B. F., 2000, preprint (astro-ph/0012117)
- Metzler, C. A., & Evrard, A. E. 1994, ApJ, 437, 564
- Nakamura, T. T., & Suto, Y. 1997, Prog. Theor. Phy., 97, 49
- Navaro, J. F., Frenk, C. S., & White, S. D. M. 1996, ApJ, 462, 563
- Navaro, J. F., Frenk, C. S., & White, S. D. M. 1997, ApJ, 490, 493
- Nichol, R. C., Romer, A. K., Holden, B. P., Ulmer, M. P., Pildis, R. A., Adami, C., Merrelli, A. J., Burke, D. J., & Collins, C. A. 1999, ApJ, 521, L21
- Nusser, A. & Sheth, R. K. 1999, MNRAS, 303, 685
- Press, W. H., & Schechter, P. 1974, ApJ, 187, 425 (PS)
- Rosati, P., Della Ceca, R., Norman, C., & Giacconi, R. 1998, ApJ, 492, L21
- Salvador-Solé, E., Solanes, J. M., & Manrique, A. 1998, ApJ, 499, 542 (SSM)
- Scharf, C. A., & Mushotzky, R. F. 1997, ApJ, 485, L65
- Tomita, K. 1969, Prog. Theor. Phys., 42, 9
- Valageas, P., & Silk, J. 1999, A&A, 350, 725
- Wu, K. K. S., Fabian, A. C., and Nulsen, P. E. J. 2000, MNRAS, 318, 889

This preprint was prepared with the AAS  $IAT_EX$  macros v5.0.

Fig. 1.— Formation redshift distribution function,  $\Phi(z_f; M, z = 0)$ , for several values of the present halo mass in (a) the SCDM model and (b) the LCDM model.

Fig. 2.— Halo mass at the formation redshift,  $M_f(z_f; M = 10^{15} M_{\odot})$ , in the SCDM model and the LCDM model.

Fig. 3.— Temperature function at z = 0 and z = 1 in (a) the SCDM model and (b) the LCDM model. Symbols indicate the predictions based on the PS formalism, while thin lines indicate the predictions based on the SSM formalism. Thick line represents the power-law fit to the observed low redshift temperature function obtained by Henry (2000).

Fig. 4.— The temperature-formation redshift relation:  $T = T(z_f; M = 10^{15} M_{\odot})$ . Thin lines are the relation in the scaling model, while thick lines are the relations in the preheating model.

Fig. 5.— Luminosity function at z = 0 and z = 1 in (a) the SCDM and (b) the LCDM. Symbols indicate the predictions based on the PS formalism, while thin lines indicate the prediction based on the SSM formalism. Thick line represents the best-fitting Schechter function to the observed bolometric luminosity function for galaxy clusters within z = 0.3 obtained by Ebeling et al. (1997).

Fig. 6.— The luminosity-formation redshift relation:  $L = L(z_f; M = 10^{15} M_{\odot})$ . This lines are the relation in the scaling model, while thick lines are the relations in the preheating model.

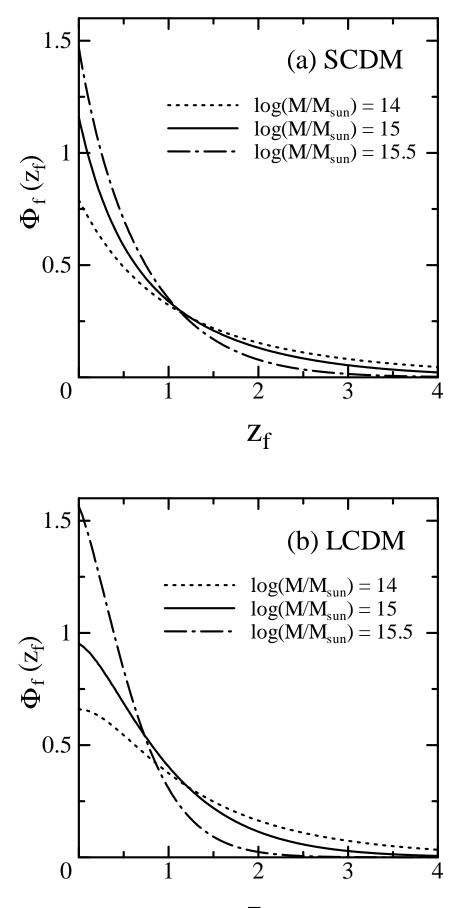
Fig. 7.— Iso-density contours on L - T plane in (a) the SCDM model and (b) the LCDM model. The values of  $\log\{n[\log(T), \log(L); z = 0]\}$  are separated at equal logarithmic intervals by 1.25 and range from -4 to -12.75. Thick line indicates the predicted L - T relation based on the PS formalism. This corresponds to the case  $z_f = 0$  and follows  $L \propto T^2$ . Dotted line represents the power-law fit to the observed L - T relation obtained by obtained by David et al. (1993). Fig. 8.— Temperature function in the preheating model at z = 0 and z = 1 in (a) the SCDM model and (b) the LCDM model. Thick line represents the power-law fit to the observed low redshift temperature function obtained by Henry (2000).

Fig. 9.— Luminosity function in the preheating model at z = 0 and z = 1 in (a) the SCDM model and (b) the LCDM model. Thick line represents the best-fitting Schechter function to the observed bolometric luminosity function within z = 0.3 obtained by Ebeling et al. (1997).

Fig. 10.— Iso-density contours on the L - T plane in (a) the SCDM model and (b) the LCDM model. The values of  $\log\{n[\log(T), \log(L); z = 0]\}$  are separated at equal logarithmic intervals by 1.25 and range from -4 to -12.75. Thick line indicates the predicted L - T relation based on the PS formalism. This corresponds to the case of  $z_f = 0$ . Dotted line represents the power-law fit to the observed L - T relation obtained by obtained by David et al. (1993).

Table 1: Cosmological parameters of the models

Model	$\Omega_0$	$\lambda_0$	h	$\sigma_8$
SCDM	1.0	0.0	0.5	1.0
LCDM	0.3	0.7	0.7	1.0



Z<sub>f</sub>

